ESAIM: PROCEEDINGS AND SURVEYS, September 2014, Vol. 45, p. 523-532
J.-S. Dhersin, Editor

A RELAXATION SCHEME FOR INVISCID FLOWS UNDER GRAVITATIONAL INFLUENCE

Jeaniffer Vides[1], Edouard Audit[2] and Boniface Nkonga[3]

Abstract. Many astrophysical flows are modeled by the Euler equations with gravity source terms derived from a potential, the evolution of which is described by a Poisson equation. Several gravitational flows reach equilibrium states that are necessary to preserve in the numerical formulation. In this paper, we present the derivation of the relaxation model [17], in which the pressure is a supplementary variable and the Poisson equation is transformed into a hyperbolic equation with a penalty parameter. The corresponding scheme is obtained in the limit as the parameter tends to zero. The proposed Riemann solver, implemented in the software HERACLES [10], provides better robustness compared to other approaches available in the same software and is capable of preserving gravitational equilibria when required. Several numerical tests and results are presented, as well.

Résumé. De nombreux écoulements en astrophysique sont modélisés par les équations d'Euler avec des termes sources de gravité dérivant d'un potentiel dont l'évolution est décrite par une équation de Poisson. Certains écoulements gravitationnels développent des états d'équilibre qu'il est nécessaire de préserver dans la formulation numérique. Nous présentons ici la dérivation du modèle de relaxation [17], dans lequel la pression est une variable complémentaire et l'équation de Poisson est transformée en une équation hyperbolique avec un paramètre de pénalisation. Le schéma est obtenu à la limite quand ce paramètre tend vers zéro. Le solveur de Riemann proposé, mis en œuvre dans la plate-forme de calcul HERACLES [10], offre plus de robustesse numérique par rapport aux précédentes approches disponibles dans la plate-forme et permet de préserver les équilibres gravitationnels lorsque le problème l'exige. Des tests et des résultats numériques sont ainsi présentés.

1. Introduction

Numerous astrophysical flows under the influence of gravity can be described by the Euler-Poisson model, given by the following system of nonlinear partial differential equations (PDEs):

$$\begin{cases} \partial_t \rho & + & \nabla \cdot (\rho \mathbf{u}) & = & 0, \\ \partial_t (\rho \mathbf{u}) & + & \nabla \cdot (\rho \mathbf{u} \otimes \mathbf{u}) + \nabla p & = & -\rho \nabla \phi, \\ \partial_t (\rho E) & + & \nabla \cdot ((\rho E + p)\mathbf{u}) & = & -\rho \mathbf{u} \cdot \nabla \phi, \\ \Delta \phi = 4\pi G \rho, & & & & \end{cases} \tag{1}$$

[1] Inria, Maison de la Simulation, USR 3441, Gif-sur-Yvette, France. e-mail: jeaniffer-lissette.vides_higueros@inria.fr
[2] CEA, Maison de la Simulation, USR 3441, Gif-sur-Yvette, France. e-mail: edouard.audit@cea.fr
[3] Université de Nice-Sophia Antipolis, UMR CNRS 7351 & Inria Sophia Antipolis, France. e-mail: boniface.nkonga@unice.fr

Article published online by EDP Sciences and available at http://www.esaim-proc.org or http://dx.doi.org/10.1051/proc/201445054

where $\rho > 0$ is the density, $\mathbf{u} \in \mathbb{R}^d$ the d-dimensional velocity, E the total specific energy, and ϕ the gravitational potential. The universal gravitational constant G is approximately equal to $6.67 \times 10^{-11} m^3 kg^{-1} s^{-2}$, and the pressure p is governed by an equation of state of the form $p = p(\rho, \epsilon)$, with $\epsilon = E - |\mathbf{u}|^2/2$ representing the specific internal energy. We assume the pressure law satisfies

$$\partial_\rho p(\rho, \epsilon) + \frac{p(\rho, \epsilon)}{\rho^2} \partial_\epsilon p(\rho, \epsilon) > 0.$$

For simplicity of notation, system (1) can also be written in condensed form as

$$\begin{cases} \partial_t \mathbf{W} + \nabla \cdot \mathbf{F}(\mathbf{W}) + \mathbf{B}(\mathbf{W}) \nabla \phi = 0, \\ \Delta \phi = 4\pi G \rho, \end{cases} \tag{2}$$

with

$$\mathbf{W} = \begin{pmatrix} \rho \\ \rho \mathbf{u} \\ \rho E \end{pmatrix}, \quad \mathbf{F}(\mathbf{W}) = \begin{pmatrix} \rho \mathbf{u}^T \\ \rho \mathbf{u} \otimes \mathbf{u} + p\, \mathcal{I}_d \\ (\rho E + p) \mathbf{u}^T \end{pmatrix}, \quad \mathbf{B}(\mathbf{W}) = \rho \begin{pmatrix} \mathbf{0}_d^T \\ \mathcal{I}_d \\ \mathbf{u}^T \end{pmatrix}, \tag{3}$$

where $\mathcal{I}_d$ is a d-dimensional identity matrix and $\mathbf{0}_d$ is the null vector in $\mathbb{R}^d$. Here, $\mathbf{W} : \mathbb{R}^d \times \mathbb{R}^+ \to \Omega_d$ is the state vector, $\mathbf{F} : \Omega_d \to \mathcal{M}_{2+d,d}(\mathbb{R})$ is the flux function, and $\mathbf{B} : \Omega_d \to \mathcal{M}_{2+d,d}(\mathbb{R})$ represents the gravitational contribution when multiplied by the gradient of the gravitational potential. We define the convex set of admissible states by

$$\Omega_d = \left\{ \mathbf{W} \in \mathbb{R}^{2+d};\ \rho > 0,\ \mathbf{u} \in \mathbb{R}^d,\ \epsilon = E - \frac{|\mathbf{u}|^2}{2} > 0 \right\}. \tag{4}$$

The above system is completed with appropriate initial and boundary conditions. For the former, we define the initial data $\mathbf{W}(\mathbf{x}, 0) = \mathbf{W}^0(\mathbf{x})$ and $\phi(\mathbf{x}, 0) = \phi^0(\mathbf{x})$.

In the field of astrophysical fluid dynamics, gas flows under gravitational influence are frequently found. In view of numerical simulations, the proper treatment of gravitational effects and the need to preserve the equilibrium states of these flows, present two major challenges. The authors in [17], use an operator splitting approach, and in the context of the first-order decomposition, solve system (2) in two steps. First, being $\mathbf{W} \in \Omega_d$ an unknown state vector and ϕ a given gravitational potential, the following nonlinear hyperbolic system is solved:

$$\partial_t \mathbf{W} + \nabla \cdot \mathbf{F}(\mathbf{W}) + \mathbf{B}(\mathbf{W}) \nabla \phi = 0. \tag{5}$$

The second step then consists in using the element ρ of the obtained solution $\mathbf{W}$ to solve the elliptic Poisson equation by means of a classical second-order finite difference approach.

Now, in order to approximate equation (5), which is in nonconservative form, Vides et al. [17] introduce the discretization of the gravity source term into the approximate Riemann solver for the Euler equations by means of a relaxation technique, a classical numerical approach widely spread across the literature considering fluid flow simulations (see [1, 6]). In this paper, we present the complete derivation of their one-dimensional relaxation model. Although the associated scheme is not well-balanced in the sense of [3, 4], we demonstrate its ability to capture and preserve steady, as well as perturbed quasi-steady, state solutions with various numerical tests. Moreover, we show the method's applicability to different types of problems under gravitational influence.

This paper is organized as follows. In Section 2, we detail the derivation of the one-dimensional relaxation model used to approximate the solutions of the system introduced at the beginning of this paper. The main steps of the associated relaxation scheme are then recalled in Section 3 and several numerical tests are presented and discussed in Section 4. Finally, concluding remarks are given in the last section.

2. Derivation of the one-dimensional relaxation model

In this section, we consider the numerical approximation of the hyperbolic-elliptic coupled system (2). Following a strategy similar to that employed in [11,12] to obtain the constrained formulation of Maxwell's equations and in [2] to couple the divergence-free constraint on the magnetic field with the ideal magnetohydrodynamic equations, we introduce a new parameter $c_h \geq 0$ and transform the elliptic equation $\nabla \cdot \nabla\phi = 4\pi G\rho$ to an approximated hyperbolic system with an augmented variable $\boldsymbol{\kappa} \approx \nabla\phi$. Thus, we get

$$\left\{\begin{array}{lcll} \partial_t \rho & + & \nabla \cdot (\rho \mathbf{u}) & = 0, \\ \partial_t (\rho \mathbf{u}) & + & \nabla \cdot (\rho \mathbf{u} \otimes \mathbf{u}) + \nabla p + \rho \nabla \phi & = 0, \\ \partial_t (\rho E) & + & \nabla \cdot ((\rho E + p)\mathbf{u}) + \rho \mathbf{u} \cdot \nabla \phi & = 0, \\ \frac{1}{c_h}\partial_t \phi & + & \nabla \cdot \boldsymbol{\kappa} & = -c_h \int_0^t 4\pi G\rho \, \mathrm{d}\tau, \\ \frac{1}{c_h}\partial_t \boldsymbol{\kappa} & + & \nabla \phi & = 0. \end{array}\right. \tag{6}$$

This reformulated system is globally hyperbolic with a source term under integral form. For sufficiently smooth solutions, combining the last two equations of this system yields the nonhomogenous wave equation

$$\frac{1}{c_h^2}\partial_{tt}\phi - \nabla \cdot \nabla\phi = 4\pi G\rho. \tag{7}$$

Note that when the parameter c_h tends towards zero, we formally recover both that $\partial_{tt}\phi = \mathcal{O}(c_h^2)$ and $\nabla \cdot \nabla\phi = 4\pi G\rho + \mathcal{O}(c_h^2)$. For the moment, we only assume that $c_h \ll 1$.

We now focus on the numerical approximation of system (6). For the sake of mathematical simplicity, we begin our analysis by considering the one-dimensional subsystem

$$\left\{\begin{array}{lcll} \partial_t \rho & + & \partial_x(\rho u) & = 0, \\ \partial_t (\rho u) & + & \partial_x(\rho u^2 + p) + \rho \partial_x \phi & = 0, \\ \partial_t (\rho E) & + & \partial_x((\rho E + p)u) + \rho u \partial_x \phi & = 0, \end{array}\right. \tag{8}$$

with $\mathbf{W} = (\rho, \rho u, \rho E)^T \in \Omega_1$. As mentioned in the previous section, particular attention must be given to the proper discretization of the gravity terms. After the work of Jin-Xin [6] and Bouchut [1], Vides et al. [17] proposed to approximate the weak solutions of (8) by the weak solutions of a relaxation system, designed to preserve most of the nonlinearities of the relaxation equilibrium system and in this way, enforce accuracy of the resulting numerical scheme. In the following, we recall some of the main ideas described in [17].

First, after the influential work of Suliciu [13,14], the pressure p is relaxed with an approximation π governed by an adequate evolution equation supplemented by a relaxation source term. From the commonly known pressure equation $\partial_t p + u\partial_x p + \rho c^2 \partial_x u = 0$, with the sound speed c satisfying $c^2 = \partial_\rho p(\rho, \epsilon) + \frac{p(\rho,\epsilon)}{\rho^2}\partial_\epsilon p(\rho, \epsilon) > 0$, it is suggested to define the evolution law

$$\partial_t \pi + u\partial_x \pi + \frac{a^2}{\rho}\partial_x u = \frac{1}{\delta}(p - \pi), \tag{9}$$

to govern the additional variable π. As the parameter δ tends to zero, a relaxation equilibrium limit characterized by $\pi = p$ is reached. It is also evident that the choice of a plays an important role in the robustness of the scheme, as will be seen in Section 4. In addition, a relaxation procedure to approximate the potential ϕ is proposed in [17], but its derivation is not given therein. Here, we present it in more detail. First, we write the last two equations of the integro-differential system (6) in their one-dimensional form

$$\left\{\begin{array}{lcll} \partial_t \phi & + & c_h \partial_x \kappa & = -c_h^2 \int_0^t 4\pi G\rho \, \mathrm{d}\tau, \\ \partial_t \kappa & + & c_h \partial_x \phi & = 0, \end{array}\right. \tag{10}$$

and their combination (see equation (7)) as $\frac{1}{c_h^2}\partial_{tt}\phi - \partial_{xx}\phi = 4\pi G\rho$. The relaxation system, which ensures adequate coupling of the Poisson and Euler equations, is then

$$\left\{\begin{array}{lcll} \partial_t\rho & + & \partial_x(\rho u) & = 0, \\ \partial_t(\rho u) & + & \partial_x(\rho u^2+\pi) + \rho\partial_x\phi & = 0, \\ \partial_t(\rho E) & + & \partial_x((\rho E+\pi)u) + \rho u\partial_x\phi & = 0, \\ \partial_t\pi & + & u\partial_x\pi + \frac{a^2}{\rho}\partial_x u & = \frac{1}{\delta}(p-\pi), \\ \partial_t\phi & + & c_h\partial_x\kappa & = -c_h^2\int_0^t 4\pi G\rho\,\mathrm{d}\tau, \\ \partial_t\kappa & + & c_h\partial_x\phi & = 0, \end{array}\right. \tag{11}$$

which can be put in the form $\partial_t\overline{\mathbf{W}} + \partial_x\overline{\mathbf{F}} + \overline{\mathbf{B}}\partial_x\phi = \frac{1}{\delta}\overline{\mathbf{R}} + c_h\overline{\mathbf{Q}}$, with $\overline{\mathbf{W}} = (\rho, \rho u, \rho E, \rho\pi, \phi, \kappa)^T$ and, after a change of variables, as $\partial_t\overline{\mathbf{V}} + \mathbf{A}\partial_x\overline{\mathbf{V}} = \frac{1}{\delta}\mathbf{S}_0 + c_h\mathbf{S}_1$, where $\overline{\mathbf{V}} = (\rho, u, \epsilon, \pi, \phi, \kappa)^T$. We note that the matrix $\mathbf{A}$ is diagonalizable and with real eigenvalues $\pm c_h, u, u \pm a/\rho$. We assume that $c_h \ll 1$ and $c_h \leq |u|$.

The method described in [17] consists of considering equations (10) in the limit $c_h = 0$. In this asymptotic case, we obtain $\partial_t\phi = 0$ and $\partial_{xx}\phi = 4\pi G\rho$, consistent with the first-order decomposition described in Section 1. We then suggest to relax the gravitational potential ϕ by replacing it with new variable ψ such that

$$\partial_t\psi = \frac{1}{\delta}(\phi - \psi), \tag{12}$$

and we write the complete relaxation model corresponding to subsystem (8) as

$$\left\{\begin{array}{lcll} \partial_t\rho & + & \partial_x(\rho u) & = 0, \\ \partial_t(\rho u) & + & \partial_x(\rho u^2+\pi) + \rho\partial_x\psi & = 0, \\ \partial_t(\rho E) & + & \partial_x((\rho E+\pi)u) + \rho u\partial_x\psi & = 0, \\ \partial_t(\rho\pi) & + & \partial_x((\rho\pi+a^2)u) & = \frac{\rho}{\delta}(p-\pi), \\ \partial_t\psi & & & = \frac{1}{\delta}(\phi-\psi). \end{array}\right. \tag{13}$$

Let us stress out that as δ tends to zero, $\pi = p$ and $\phi = \psi$, and the evolution equations for $(\rho, \rho u, \rho E)^T$ are thus equivalently to those found in system (8). Moreover, defining $\mathbf{W}_\delta = (\rho, \rho u, \rho E, \rho\pi, \psi)^T \in \Omega_\delta$, with Ω_δ the set of admissible relaxation state vectors given by

$$\Omega_\delta = \left\{\mathbf{W}_\delta \in \mathbb{R}^5;\ \rho > 0,\ u \in \mathbb{R},\ \epsilon = E - \frac{u^2}{2} > 0,\ \pi \in \mathbb{R},\ \psi \in \mathbb{R}\right\},$$

we propose a compact form representation of (13) in the following way:

$$\partial_t\mathbf{W}_\delta + \partial_x\mathbf{F}_\delta(\mathbf{W}_\delta) + \mathbf{B}_\delta(\mathbf{W}_\delta)\partial_x\psi = \frac{1}{\delta}\mathbf{R}_\delta(\mathbf{W}_\delta), \tag{14}$$

with

$$\begin{aligned} \mathbf{F}_\delta(\mathbf{W}_\delta) &= \left(\rho u, \rho u^2+\pi, (\rho E+\pi)u, \left(\rho\pi + a^2\right)u, 0\right)^T, \\ \mathbf{B}_\delta(\mathbf{W}_\delta) &= (0, \rho, \rho u, 0, 0)^T, \\ \mathbf{R}_\delta(\mathbf{W}_\delta) &= (0, 0, 0, \rho(p-\pi), \phi-\psi)^T. \end{aligned}$$

3. One-dimensional relaxation scheme

Based on the model described in the previous section, we now present the main steps involved in the numerical time-update strategy employed to approximate the solution of the initial value problem

$$\begin{cases} \partial_t \mathbf{W} + \partial_x \mathbf{F}(\mathbf{W}) + \mathbf{B}(\mathbf{W})\partial_x \phi = 0, \\ \partial_{xx}\phi = 4\pi G\rho, \\ \mathbf{W}(x,0) = \mathbf{W}^0(x), \;\; \phi(x,0) = \phi^0(x). \end{cases} \tag{15}$$

As mentioned in the previous sections, we use a first-order operator splitting approach to decompose (15) into two subsystems: the Euler equations with gravity source terms and the Poisson equation. We consider a uniform numerical grid with N_x cells of size $\Delta x = x_{i+1/2} - x_{i-1/2}$ $(i = 1, ..., N_x)$. The time increment is given by Δt such that $t^{n+1} = t^n + \Delta t$ for $n \in \mathbb{N}$.

3.1. Euler equations with gravity source terms

In this step, $\mathbf{W}$ is the unknown vector and the gravitational potential ϕ is an *a priori* given function.

3.1.1. *Evolution in time ($\delta = \infty$)*

At the beginning of the time step t^n, we construct the initial data

$$\mathbf{W}_\delta^h(x,t^n) = (\rho_i^n,\;(\rho u)_i^n,\;(\rho E)_i^n,\;(\rho\pi)_i^n = \rho_i^n p_i^n,\quad \psi_i^n = \phi_i^n)\,, \qquad x \in \left(x_{i-1/2}, x_{+1/2}\right), \tag{16}$$

which coincides with a relaxation equilibrium state as $\pi_i^n = p_i^n$ and $\psi_i^n = \phi_i^n$ are set. Then, for all $t \in (0, \Delta t)$, we look for the weak solutions $\mathbf{W}_\delta^h(x, t^n + t)$ of the Cauchy problem

$$\partial_t \mathbf{W}_\delta + \partial_x \mathbf{F}_\delta(\mathbf{W}_\delta) + \mathbf{B}_\delta(\mathbf{W}_\delta)\partial_x \psi = 0, \tag{17}$$

subject to the previously defined initial data $\mathbf{W}_\delta^h(x, t^n)$. We wish to point out that equation (17) is the relaxation model (14) without the source terms, *i.e.*, with $\delta = \infty$. Now, the solution $\mathbf{W}_\delta^h(x, t^n + t)$ is approximated as a superposition of non-interacting Riemann solutions emerging at each interface $x_{i+1/2}$ for positive times t less than Δt, satisfying the restriction

$$\frac{\Delta t}{\Delta x} \max_{i\in\mathbb{Z}} \left(|\mu^-_{i+\frac{1}{2}}|, |\mu^+_{i-\frac{1}{2}}| \right) \leq \frac{1}{2}, \tag{18}$$

where $\mu^-_{i+1/2}$ and $\mu^+_{i+1/2}$ are estimates of the slowest and fastest wave speeds, respectively. In [17], the authors present the Riemann solution $\mathcal{W}_\delta^{\mathcal{R}}$ for the relaxation model (17). Simultaneously, relevant choices of the parameter a are specified to enforce a suitable positive preserving property. Here, in this paper, given two constant states $(\mathbf{W}_\delta)_i^n$ and $(\mathbf{W}_\delta)_{i+1}^n$ separated by a discontinuity at $x_{i+1/2}$, we define this parameter a locally at each interface as

$$a_{i+1/2} = a_0 \max\left(\rho_i^n c_i^n, \rho_{i+1}^n c_{i+1}^n\right), \tag{19}$$

with a_0 a positive constant, the value of which is fixed according to the specific physical settings of the problem addressed so all robustness conditions described in Section 3 of [17] are satisfied. Unless specified otherwise, we use $a_0 = 1.05$ for our numerical simulations. Thus, we write

$$\mathbf{W}_\delta^h(x, t^n + t) = \mathcal{W}_\delta^{\mathcal{R}}\left(\frac{x - x_{i+1/2}}{t}; (\mathbf{W}_\delta)_i^n, (\mathbf{W}_\delta)_{i+1}^n, a_{i+1/2}\right), \qquad x \in (x_i, x_{i+1}),\;\; t \in (0, \Delta t).$$

Let us note that because of the potential source term, the standard conservative flux balance cannot be reached. However, making use of the formalism introduced by Harten, Lax and van Leer [5], we define

$$(\mathbf{W}_\delta)_i^{n+1,-} = (\mathbf{W}_\delta)_i^n - \frac{\Delta t}{\Delta x}\left(\mathbf{F}_\delta^L((\mathbf{W}_\delta)_i^n, (\mathbf{W}_\delta)_{i+1}^n) - \mathbf{F}_\delta^R((\mathbf{W}_\delta)_{i-1}^n, (\mathbf{W}_\delta)_i^n)\right), \tag{20}$$

where

$$\begin{aligned}\mathbf{F}_\delta^L((\mathbf{W}_\delta)_i^n,(\mathbf{W}_\delta)_{i+1}^n) =& \mathbf{F}_\delta((\mathbf{W}_\delta)_i^n) \\ &- \frac{1}{\Delta t}\int_{x_i}^{x_{i+\frac{1}{2}}} \left(\mathcal{W}_\delta^{\mathcal{R}}\left(\frac{x-x_{i+\frac{1}{2}}}{\Delta t};(\mathbf{W}_\delta)_i^n,(\mathbf{W}_\delta)_{i+1}^n\right)-(\mathbf{W}_\delta)_i^n\right)dx, \qquad (21)\\ \mathbf{F}_\delta^R((\mathbf{W}_\delta)_i^n,(\mathbf{W}_\delta)_{i+1}^n) =& \mathbf{F}_\delta((\mathbf{W}_\delta)_{i+1}^n) \\ &+ \frac{1}{\Delta t}\int_{x_{i+\frac{1}{2}}}^{x_{i+1}} \left(\mathcal{W}_\delta^{\mathcal{R}}\left(\frac{x-x_{i+\frac{1}{2}}}{\Delta t};(\mathbf{W}_\delta)_i^n,(\mathbf{W}_\delta)_{i+1}^n\right)-(\mathbf{W}_\delta)_{i+1}^n\right)dx. \qquad (22)\end{aligned}$$

3.1.2. *Relaxation equilibrium ($\delta = 0$)*

This step of the scheme consists in solving $\partial_t \mathbf{W}_\delta = \frac{1}{\delta}\mathbf{R}_\delta(\mathbf{W}_\delta)$, with initial data defined by the piecewise constant approximation $(\mathbf{W}_\delta)_i^{n+1,-}$. As $\delta \to 0$, the updated approximate equilibrium solution is then given by

$$\mathbf{W}_i^{n+1} = \left(\rho_i^{n+1,-},(\rho u)_i^{n+1,-},(\rho E)_i^{n+1,-}\right)^T, \qquad (23)$$

and we enforce $\pi_i^{n+1} = p_i^{n+1}$ and $\psi_i^{n+1} = \phi_i^{n+1}$ to recover a relaxation equilibrium.

3.2. **Poisson equation**

This second step consists in using the first component of $\mathbf{W}_i^{n+1}$, i.e., ρ_i^{n+1}, to solve the Poisson equation and thus obtain ϕ_i^{n+1}. The discretization of $\partial_{xx}\phi = 4\pi G\rho$ by means of a second-order finite difference approach, yields a tridiagonal matrix. The resulting matrix equation is then solved by using direct or iterative methods.

4. Numerical results

The relaxation strategy presented in the previous section is implemented in the code HERACLES [10], and here, it is applied in three different situations. Unless stated otherwise, the thermodynamic pressure p is assumed to be governed by an ideal equation of state $p = (\gamma - 1)\rho\epsilon$, with the specific heat capacity ratio $\gamma = 1.4$. For second-order approximations, we extend the scheme by using the MUSCL-Hancock Method (MHM), see [15], and as for the choice of slope limiters, we use the MC limiter [16]. Let us note though that no slope is used for the gravitational potential in order to have a proper potential jump at each cell interface, as is also done in [9].

When needed, the relaxation scheme is compared with the standard fractional step splitting method (hereafter referred to as the *standard method*) implemented in HERACLES. This is a known and simple approach in which equation (5) is solved by splitting it into

$$\begin{aligned}\partial_t \mathbf{W} + \nabla\cdot\mathbf{F}(\mathbf{W}) &= 0,\\ \partial_t \mathbf{W} &= -\mathbf{B}(\mathbf{W})\nabla\phi.\end{aligned} \qquad (24)$$

4.1. **Sod shock tube under gravitational influence**

As a first test, we consider the Sod shock tube problem under a gravitational field, as described in [9, 18]. The main advantage of this test is that it consists of a relatively simple initial setup, summarized in Table 1. The test is then run to time $t = 0.2$ on a coarse grid composed of 100 cells using the relaxation scheme presented in Section 3. Figure 1 shows the corresponding density, velocity, pressure, and total energy density plots, compared with a reference solution computed on a refined grid of 4000 cells. Due to the existence of a gravitational field, the first plot in the series shows how the density profile is pushed towards the left and the velocity plot reveals the development of negative velocities. As expected, the first-order results are the most diffusive given that the initial discontinuities are spread out over several zones. Second-order results are clearly more accurate and satisfying, and demonstrate that the relaxation scheme is able to capture shocks correctly.

Shock Tube with Gravity

Computational domain: $[0,1]$; Reflecting boundaries				
	$\rho^0(x)$	$u^0(x)$	$p^0(x)$	Gravity potential
$x \leq 0.5$	1.000	0.0	1.0	$\phi(x) = gx$, with $g = 1.0$
$x > 0.5$	0.125	0.0	0.1	

TABLE 1. Initial data for the Sod shock tube under a gravitational field described in [9].

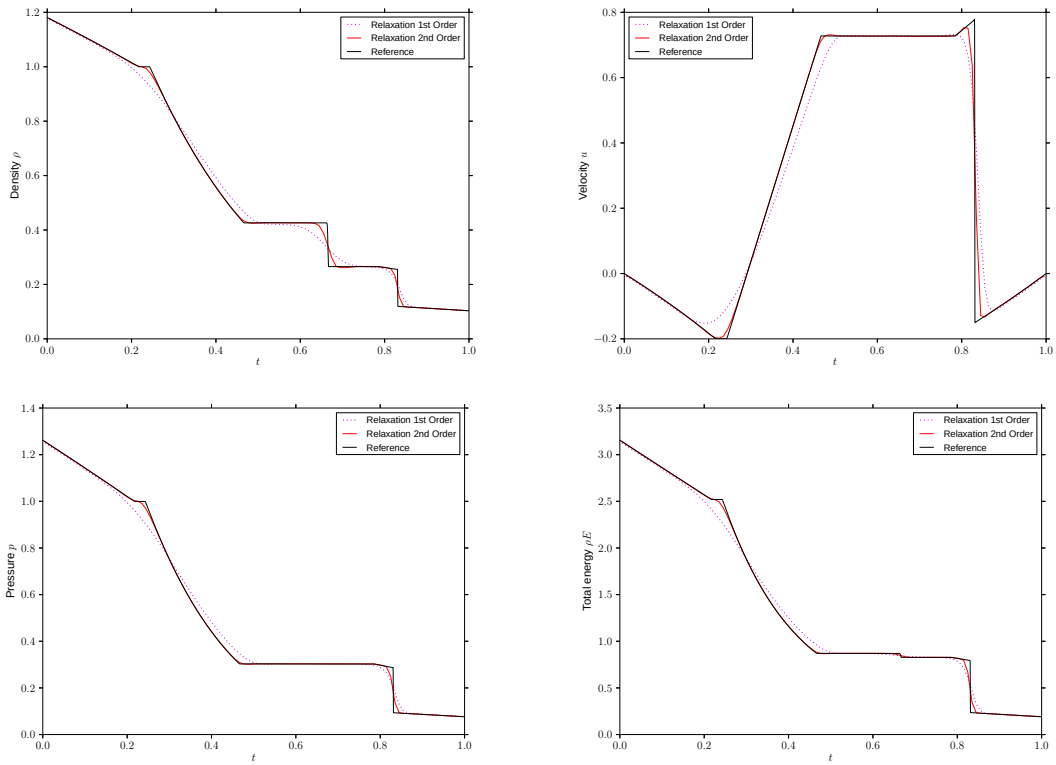

FIGURE 1. Several distributions obtained with the relaxation scheme proposed in this paper for Test 4.1 at time $t = 0.2$, using $N_x = 100$ cells and $a_0 = 1.0$. The results are compared with a reference solution obtained using the second-order algorithm on a finer grid of 4000 cells.

4.2. **Perturbed one-dimensional isothermal equilibrium**

LeVeque and Bale [8] first proposed this test to determine a method's ability to capture perturbed near-equilibrium solutions. The problem consists of an ideal gas in isothermal equilibrium. A small perturbation to the pressure is introduced and its behavior is then examined over time. The initial conditions and perturbation are given in Table 2.

The test is initialized on a computational domain $x \in [0,1]$ consisting of 100 evenly spaced cells, with the initial perturbation centered at $x = 0.5$. Two different values for the perturbation amplitude η are considered, $\eta = 0.01$ and $\eta = 0.001$. For the latter, it is demonstrated in [8] that the standard method is not able to correctly capture the perturbed pressure nor maintain the boundary values.

Perturbed Isothermal Equilibrium

Computational domain: $[0,1]$; Fixed boundary conditions			
$\rho^0(x)$	$u^0(x)$	$p^0(x)$	Gravity potential
e^{-x}	0.0	e^{-x}	$\phi(x) = gx$, with $g = 1.0$
Initial perturbed pressure: $p(x,0) = p^0(x) + \eta e^{-100(x-0.5)^2}$, with $0 < \eta \ll 1$			

TABLE 2. Initial data for the one-dimensional isothermal equilibrium described in [8].

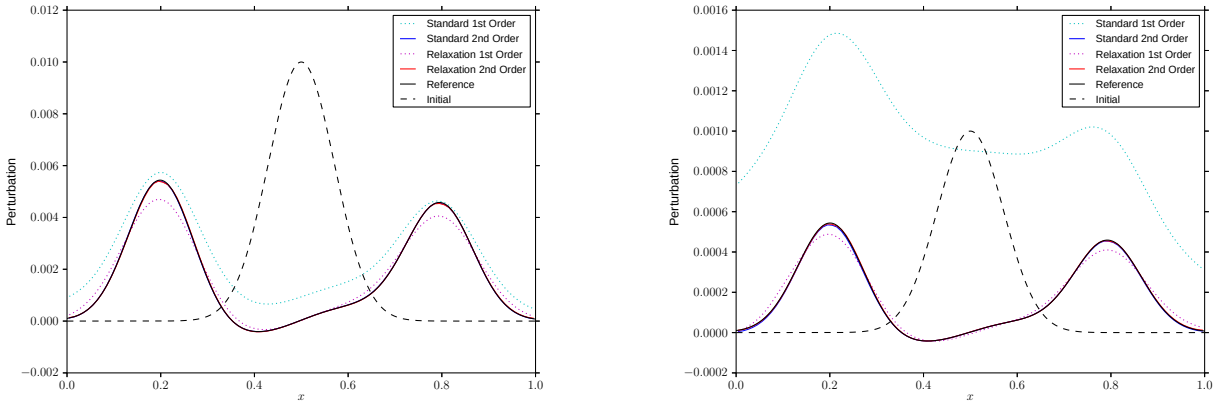

(A) $\eta = 0.01$ (B) $\eta = 0.001$

FIGURE 2. Comparison of the standard and relaxation schemes for the perturbed isothermal equilibrium test at time $t = 0.25$ and with $N_x = 100$. For the relaxation method, $a_0 = 0.83$ and $a_0 = 2.01$ were used for first- and second-order, respectively. The solid black line gives a reference solution obtained with the second-order relaxation scheme on a finer grid consisting of 4000 zones.

We run this test and the perturbation $p(x,t) - p^0(x)$ at time $t = 0.25$ is shown in Figure 2. The perturbation at the initial time is indicated by the dashed line and the reference solution obtained with the second-order relaxation method using a higher resolution is included with a solid black line. Second-order results show that both methods implemented in HERACLES [10] are able to capture the correct solution. First-order results are more dissipative and we can perceive that the standard method fails to capture the perturbation, specially when $\eta = 0.001$, as seen on the left of Figure 2. The advantages of our numerical scheme are then adequately demonstrated by performing this test.

4.3. **Equilibrium of a self-gravitating compressible fluid**

In this context, we rewrite system (1) in spherical coordinates (r, θ, φ), assuming rotational invariance around the axes e_θ and e_φ, and obtain

$$\begin{cases} \partial_t \rho + \dfrac{1}{r^2}\partial_r(r^2 \rho u_r) = 0, \\ \partial_t(\rho u_r) + \dfrac{1}{r^2}\partial_r(r^2 \rho u_r^2) + \partial_r(p) = -\rho \partial_r(\phi), \\ \dfrac{1}{r^2}\partial_r\left(r^2 \partial_r \phi\right) = 4\pi G \rho. \end{cases} \tag{25}$$

Let us consider a self-gravitational fluid at hydrostatic equilibrium, i.e., $\partial_t = 0$ and $u_r = 0$, governed by the polytropic equation of state $p = \kappa\rho^\gamma = \kappa\rho^{1+\frac{1}{n}}$, where κ is the polytropic constant, γ the adiabatic exponent and n the polytropic index. Interestingly, this equilibrium flow can be characterized by the *Lane-Emden equation* [7], thoroughly described in [17].

Self-Gravitational Fluid at Hydrostatic Equilibrium - $n = 1$

Computational domain: $[0, L_r]$ with $L_r = 6.0 \times 10^5$; Fixed boundary conditions				
ρ_c	$\rho^0(r)$	$u_r^0(r)$	$p^0(r)$	Gravity potential
10.0	$\rho_e(r)$	0.0	$\kappa\,(\rho_e(r))^2$	$\phi^0(r) = -2\kappa\,\rho_e(r)$
Solution to the *Lane-Emden equation*: $\rho_e(r) = \rho_c * sin(z)/(z)$ with $z = A\,r = \sqrt{4\pi G/(2\kappa)}\,r$				

TABLE 3. Initial data for the self-gravitational fluid at hydrostatic equilibrium described in [17] with the polytropic constant $\kappa = 1000$.

We then propose to validate the relaxation method with a polytropic gas of index $n = 1$. Its initial state is summarized in Table 3, where the central density is denoted by ρ_c. The number of grid cells is set to 100 and the final time of the experiment to 1.0×10^7. Note that the evolution of the potential is described by the Poisson equation in spherical symmetry, i.e., the last equation of system (25). We solve this equation with Dirichlet boundary conditions on the one-dimensional domain by means of a standard LU method at each time step.

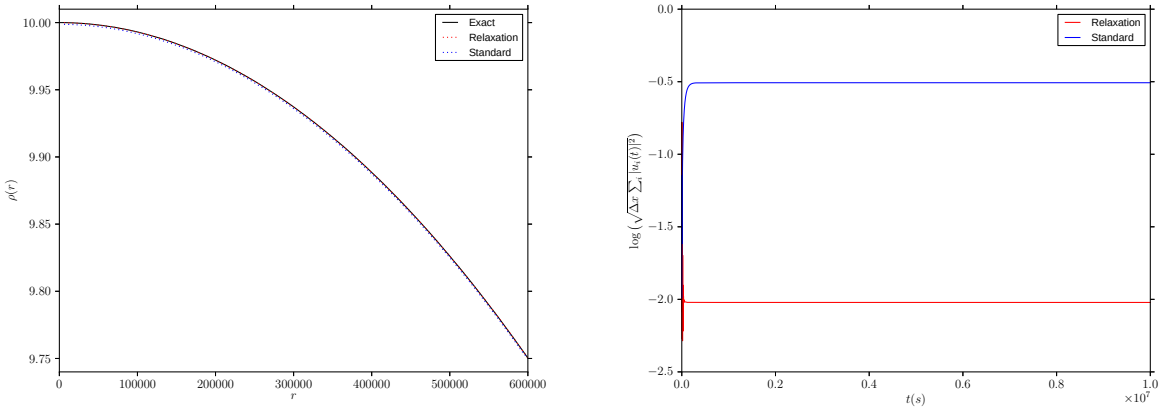

(A) Density at time $t = 1.0 \times 10^7$

(B) L^2 norm of the velocity

FIGURE 3. Comparison of the relaxation and standard schemes for the self-gravitational fluid at equilibrium, using $N_r = 100$ cells and $a_0 = 1.05$. The approximate number of time steps for this simulation is 1.065×10^7 steps, for both methods.

The numerical densities for both schemes, compared with the exact solution $\rho_e(r)$, at the final simulation time $t = 1.0 \times 10^7$ are displayed in Figure 3(a). Additionally, we observe the evolution of the parasitic currents during the simulation in Figure 3(b). This plot of the evolution in time of the L^2 norm of the velocity, in logarithmic scale, shows that the residual velocity is far lower for the relaxation method than for the standard method. Thus, the relaxation scheme enables a good approximation of equilibrium solutions since it generates very low parasitic currents.

5. Conclusions

In this paper, we have detailed the derivation of a one-dimensional relaxation model that ensures adequate coupling of the Poisson and Euler equations and yields the scheme described in [17] in the limit as the penalty parameter c_h tends to zero. Many problems of current interest require not only the preservation of equilibrium states but also robust numerical simulations. With different types of examples, we have established the scheme's robustness and demonstrated its ability to capture and preserve steady and perturbed quasi-steady states when required. Additionally, in view of astrophysical simulations, the last test case shows that the method is able to preserve the stationary regime of self-gravitational equilibrium flows.

References

[1] F. Bouchut. *Nonlinear stability of finite volume methods for hyperbolic conservation laws, and well-balanced schemes for sources*. Frontiers in Mathematics. Birkhäuser, 2004.

[2] A. Dedner, F. Kemm, D. Kröner, C.-D. Munz, T. Schnitzer, and M. Wesenberg. Hyperbolic divergence cleaning for the MHD equations. *Journal of Computational Physics*, 175(2):645–673, 2002.

[3] J.M. Greenberg and A.Y. Leroux. A well-balanced scheme for the numerical processing of source terms in hyperbolic equations. *SIAM Journal on Numerical Analysis*, 33(1):1–16, 1996.

[4] J.M. Greenberg, A.Y. LeRoux, R. Baraille, and A. Noussair. Analysis and approximation of conservation laws with source terms. *SIAM Journal on Numerical Analysis*, 34(5):1980–2007, 1997.

[5] A. Harten, P. Lax, and B. Leer. On upstream differencing and Godunov-type schemes for hyperbolic conservation laws. *SIAM Review*, 25(1):35–61, 1983.

[6] S. Jin and Z.P. Xin. The relaxation schemes for systems of conservation laws in arbitrary space dimensions. *Communications on Pure and Applied Mathematics*, 48(3):235–276, 1995.

[7] R. Kippenhahn and A. Weigert. *Stellar structure and evolution*. Astronomy and Astrophysics Library. Springer, 1990.

[8] R.J. LeVeque and D.S. Bale. Wave propagation methods for conservation laws with source terms. In *Proceedings of the 7th International Conference on Hyperbolic Problems*, pages 609–618, 1998.

[9] J. Luo, K. Xu, and N. Liu. A well-balanced symplecticity-preserving gas-kinetic scheme for hydrodynamic equations under gravitational field. *SIAM Journal on Scientific Computing*, 33(5):2356–2381, 2011.

[10] M. González, E. Audit, and P. Huynh. HERACLES: a three-dimensional radiation hydrodynamics code. *Astronomy & Astrophysics*, 464(2):429–435, 2007.

[11] C.-D. Munz, P. Omnes, R. Schneider, E. Sonnendrücker, and U. Voß. Divergence correction techniques for Maxwell solvers based on a hyperbolic model. *Journal of Computational Physics*, 161(2):484–511, 2000.

[12] C.-D. Munz, R. Schneider, E. Sonnendrücker, and U. Voss. Maxwell's equations when the charge conservation is not satisfied. *Comptes Rendus de l'Académie des Sciences - Series I - Mathematics*, 328(5):431–436, 1999.

[13] I. Suliciu. On modelling phase transitions by means of rate-type constitutive equations. Shock wave structure. *International Journal of Engineering Science*, 28(8):829–841, 1990.

[14] I. Suliciu. Some stability-instability problems in phase transitions modelled by piecewise linear elastic or viscoelastic constitutive equations. *International Journal of Engineering Science*, 30(4):483–494, 1992.

[15] E.F. Toro. *Riemann solvers and numerical methods for fluid dynamics: a practical introduction*. Springer, 2009.

[16] B. van Leer. Towards the ultimate conservative difference scheme. IV. A new approach to numerical convection. *Journal of Computational Physics*, 23(3):276–299, 1977.

[17] J. Vides, B. Braconnier, E. Audit, C. Berthon, and B. Nkonga. A Godunov-type solver for the numerical approximation of gravitational flows. *Communications in Computational Physics*, 15(1):46–75, 2014.

[18] Y. Xing and C.-W. Shu. High order well-balanced WENO scheme for the gas dynamics equations under gravitational fields. *Journal of Scientific Computing*, 54(2-3):645–662, 2013.